To appear in *High Pressure Research*
Vol. 00, No. 00, March 2015, 1–9

Pressure dependent structure of the null-scattering alloy $Ti_{0.676}Zr_{0.324}$

Anita Zeidler[a*] Malcolm Guthrie[b†] and Philip S. Salmon[a]

[a] *Department of Physics, University of Bath, Bath BA2 7AY, UK*
[b] *Geophysical Laboratory, Carnegie Institution of Washington, Washington, DC 20015, USA*

(*March 2015*)

The room temperature structure of the alloy $Ti_{0.676}Zr_{0.324}$ was measured by x-ray diffraction under compression at pressures up to ∼30 GPa. This alloy is used as a construction material in high-pressure neutron-scattering research, and has a mean coherent neutron scattering length of zero i.e. it is a so-called 'null-scattering' alloy. A broad phase transition was observed from a hexagonal close-packed (hcp) α-phase to a hexagonal ω-phase, which started at a pressure of $\lesssim$12 GPa and was completed by ∼25 GPa. The data for the α-phase were fitted by using a third order Birch-Murnaghan equation of state, giving an isothermal bulk modulus $B_0 = 87(4)$ GPa and pressure derivative $B_0' = 6.6(8)$. The results will help to ensure that accurate structural information can be gained from *in situ* high-pressure neutron-diffraction work on amorphous and liquid materials where the $Ti_{0.676}Zr_{0.324}$ alloy is used as a gasket material.

Keywords: high pressure, equation of state, x-ray diffraction, neutron diffraction

1. Introduction

Titanium and zirconium are miscible and together they form solid solutions over the entire compositional range [1, 2]. The alloy $Ti_{0.676}Zr_{0.324}$ is an important construction material in high-pressure neutron-scattering research where it is used to make containers and gaskets [3]. One of the motivations for this choice arises from the difference in sign of the coherent neutron scattering lengths for Ti and Zr: They are −3.438(2) fm and 7.16(3) fm, respectively, so that neutrons scattered by the nuclei of these elements have opposite phases [4]. The composition of the $Ti_{0.676}Zr_{0.324}$ alloy therefore leads to a mean coherent neutron scattering length of zero i.e. it is a so-called 'null-scattering' alloy with a diffraction pattern that should be flat and featureless [5, 6]. In practice, a measured neutron diffraction pattern will, however, show some structure (Figure 1) that arises from non-ideal mixing [3, 6].

When investigating the structure of amorphous and liquid materials using *in situ* high-pressure neutron diffraction, it is essential to make an accurate correction for the attenuation and multiple scattering of a neutron beam by the gasket material. This procedure requires the number density of the gasket material under pressure [6, 10–12]. It is therefore timely to measure the equation of state for the $Ti_{0.676}Zr_{0.324}$ alloy. Here, we will use x-ray diffraction to investigate the room temperature structure of this alloy under compression at pressures up to ∼30 GPa.

*Corresponding author. Email: a.zeidler@bath.ac.uk
†Now at the European Spallation Source, ESS AB, SE-22100 Lund, Sweden

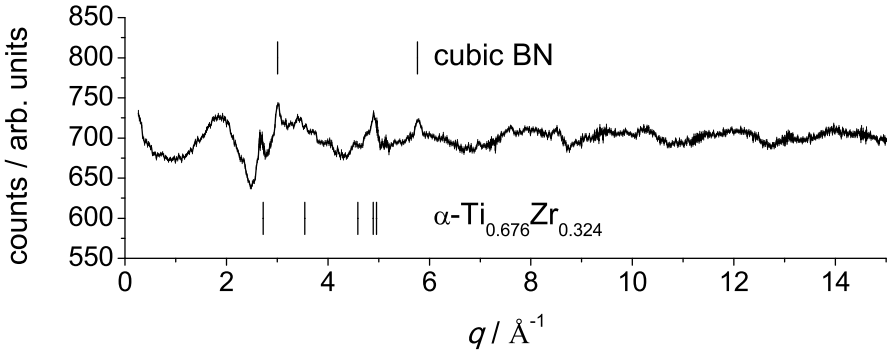

Figure 1. The neutron diffraction pattern (points with vertical error bars) measured at ambient pressure for a $Ti_{0.676}Zr_{0.324}$ gasket placed inside the cubic-BN anvils of a Paris-Edinburgh press [3] and mounted on the instrument D4c [7]. The pattern is plotted as a function of the magnitude of the scattering vector $q = (4\pi/\lambda)\sin\theta$ where 2θ is the scattering angle and λ (= 0.6947(1) Å) is the incident neutron wavelength [8]. Vertical bars mark (in ascending order) the 101, 102, 103, 112 and 201 reflections for α-$Ti_{0.676}Zr_{0.324}$ at a pressure of 1.4 GPa (corresponding to the lowest pressure data set shown in Figure 2), along with the 111 and 311 reflections for the cubic-BN anvil material at ambient conditions [9]. The diffraction pattern for the gasket alloy shows small Bragg peaks and q-dependent structure that arise from non-ideal mixing e.g. from like-atom clustering. The crystallites in the alloy often have preferred orientations [6].

2. Experimental Methods

A $Ti_{0.676}Zr_{0.324}$ billet (of composition in mass% given by Ti: 51.5 %, Zr: 48.27 %, O: 0.11 %, C: 0.008 %, N: 0.003 %, H: 0.0014 %, Hf: < 0.0035 %, Fe: 0.10 %) was formed from sponges of nuclear grade titanium and zirconium using a double vacuum-arc smelting process. Residual pores formed by gaseous inclusions were subsequently reduced, both in size and quantity, by employing the technique of hot-isostatic pressing (HIPing) [13] with argon gas as a pressurising medium at 1850 bar and a temperature of at least 1000 °C (Robert Done, ISIS facility, private communication, 2009).

A flake of swarf cut from the alloy was loaded into a screw-driven symmetric-style diamond anvil cell (DAC) together with gold powder, a ruby sphere and neon at a pressure of ∼0.2 GPa. The DAC had 330 μm culets, an inner diameter of 120 μm, and the gasket thickness at loading was in the range of 35–40 μm. Neon is a pressure-transmitting medium that provides hydrostatic conditions at pressures up to ∼15 GPa [14]. Beyond this threshold, the pressure gradients within a DAC are small, giving a <1 % pressure variation at 50 GPa [14]. Gold was intended for use as a pressure calibrant but, because of overlap with Bragg peaks from the ω-phase, ruby was used for the determination of the pressure [15] before and after each run. The mean of these pressure values is quoted for each state point, and the variation did not exceed 0.2 GPa.

X-ray diffraction patterns were collected on the 16-IDB beamline at the APS using an incident wavelength of 0.4066(1) Å. A PILATUS 1M-F detector [16] was used for data collection. The measured two-dimensional diffraction data were integrated using FIT2D [17] and were refined using the GSAS package [18]. A strained $Ti_{0.676}Zr_{0.324}$ alloy was indicated by the breadth of the measured Bragg peaks (Figure 2), even though neon was used as a pressure-transmitting medium. This strain is likely to result from the alloying process [3], but the machining procedure used to prepare the sample for the x-ray diffraction experiment may have also contributed.

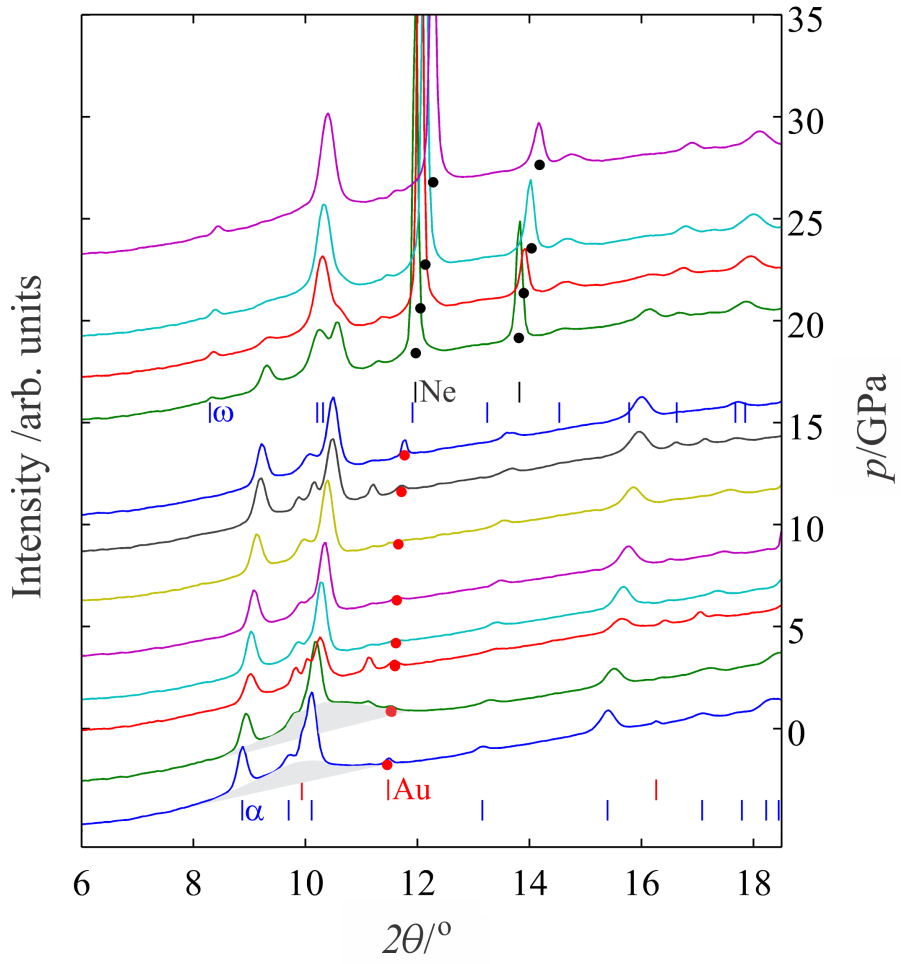

Figure 2. The pressure dependence of the x-ray diffraction patterns measured for the null-scattering alloy $Ti_{0.676}Zr_{0.324}$ at ≃24 °C. The pressures are indicated by the intercepts of these patterns with the right-hand ordinate axis. At the base pressure of 1.4 GPa, vertical bars mark (in ascending order) the 100, 002, 101, 102, 110, 103, 200, 112 and 201 reflections for α-$Ti_{0.676}Zr_{0.324}$ and the 111, 200 and 220 reflections for the gold pressure calibrant. The 111 reflections for gold cannot be resolved because they overlap with Bragg peaks from the null-scattering alloy, and the pressure dependence of the gold 200 reflections is indicated by the solid light (red) circles. At the lowest two pressures, the grey shaded areas indicate the intensity scattered from the liquid Ne pressure-transmitting medium. The signal from this medium is lost as Ne freezes into a quasi-single crystal at a pressure above 5 GPa, but the signal reappears at 20.6 GPa when the crystal is broken up. At this pressure, vertical bars mark (in ascending order) the 111 and 200 reflections for Ne and the 001, 101, 110, 200, 111, 201, 210, 002, 102 and 211 reflections for ω-$Ti_{0.676}Zr_{0.324}$. The pressure dependence of the Ne reflections is indicated by the solid dark (black) circles.

3. Results

The $Ti_{0.676}Zr_{0.324}$ alloy crystallises into a hexagonal close-packed (hcp) α-phase at ambient-pressure, as confirmed by the measured x-ray diffraction patterns (Figure 2). At a pressure of ∼12 GPa, a transformation to a hexagonal ω-phase [19] was detected, where the fraction of this phase was ≃10 %. The proportion of ω-phase increased gradually with pressure, and the $\alpha \rightarrow \omega$ phase transformation was completed by ∼24.8 GPa. In comparison, the onset pressure for the transformation from an hcp α-phase to a hexagonal ω-phase has been reported to be in the range of 2.2–6.7 GPa for Zr [19, 20], 10.7(7)–11.0(1.5) GPa for the equimolar alloy $Ti_{0.5}Zr_{0.5}$ [21, 22], and 2.9–11 GPa for Ti [23]. The onset pressure for a given material depends on factors such as the impurity

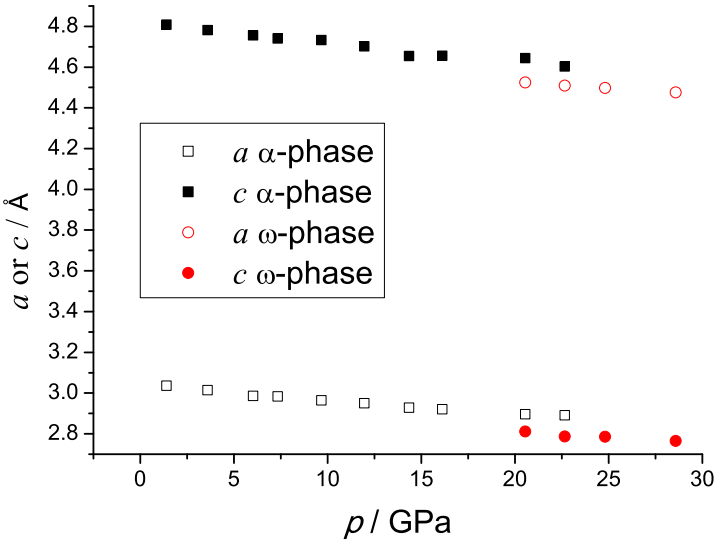

Figure 3. The pressure dependence in $Ti_{0.676}Zr_{0.324}$ of (i) the lattice parameters a (open squares) and c (closed squares) for the α-phase and (ii) the lattice parameters a (open circles) and c (closed circles) for the ω-phase. The error bars are smaller than the symbol sizes.

content and grain size of the metal, and it also depends on the pressure-transmitting medium employed in an experiment [19, 23, 24]. Coexistence of the α- and ω-phases has been reported for a pressure range of 10–13 GPa for high-purity nano-crystalline Ti using a 4:1 methanol:ethanol pressure-transmitting medium [24], and for a pressure range of 10.2–14.7 GPa (4:1 methanol:ethanol), 6.2–14.2 GPa (NaCl), 10.5–14.9 GPa (argon) or 4.9–12.4 GPa (no pressure transmitting medium) for Ti of commercial purity [23], where the spread in values corresponds to the use of different pressure-transmitting media as specified in the brackets. For the equimolar alloy $Ti_{0.5}Zr_{0.5}$, coexistence of the α- and ω-phases has been reported for a pressure range of 10.7(7)–21.6(7) GPa [22].

The pressure dependence of the lattice parameters for the α- and ω-phases of the $Ti_{0.676}Zr_{0.324}$ alloy is shown in Figure 3. The c/a lattice parameter ratio takes, within the accuracy of the measurements, a nearly constant value of 1.592(2) for the α-phase and 0.619(1) for the ω-phase (Figure 4). A near constancy of the c/a ratio with pressure has also been reported for both the α- and ω-phases of Ti [23, 25], Zr [26] and $Ti_{0.5}Zr_{0.5}$ [21], although an increase of this ratio with pressure has been reported for α-Ti [23]. In the case of the equimolar alloy $Ti_{0.5}Zr_{0.5}$, the measured c/a ratio is 1.581(5) for the α-phase and 0.618(2) for the ω-phase [21].

The pressure induced change to the atomic volume V of the $Ti_{0.676}Zr_{0.324}$ alloy is shown in Figure 5. The fractional decrease in volume between the α- and ω-phases $\Delta V/V_\alpha$, where V_α is the volume of the α-phase, is about 1.6(2)% at $\simeq$21.5 GPa, which compares to a measured value of 2.1% in the equimolar alloy $Ti_{0.5}Zr_{0.5}$ for the onset of the $\alpha \rightarrow \omega$ transition at 11 GPa [21]. The results for the α-phase were fitted by using a third order Birch-Murnaghan equation of state as written in the form [27]

$$F_E \equiv \frac{p}{3f_E\left(1+2f_E\right)^{\frac{5}{2}}} = B_0 + \frac{3B_0}{2}\left(B_0' - 4\right) f_E \qquad (1)$$

where F_E denotes a 'normalised stress', p is the pressure, $f_E \equiv \frac{1}{2}\left[\left(V_0/V\right)^{\frac{2}{3}} - 1\right]$ is the

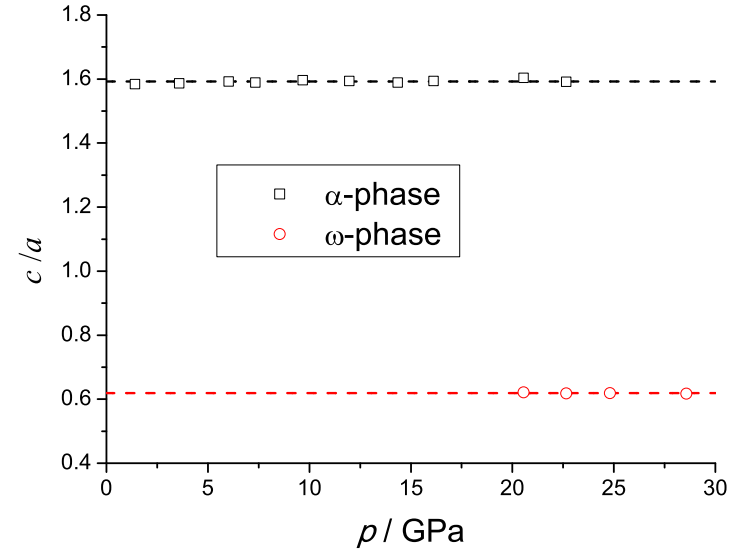

Figure 4. The pressure dependence in $Ti_{0.676}Zr_{0.324}$ of the c/a lattice parameter ratio for the α-phase [open (black) squares] and for the ω-phase [open (red) circles]. For each phase, the c/a ratio shows little variation with pressure and the average values are indicated by horizontal broken curves.

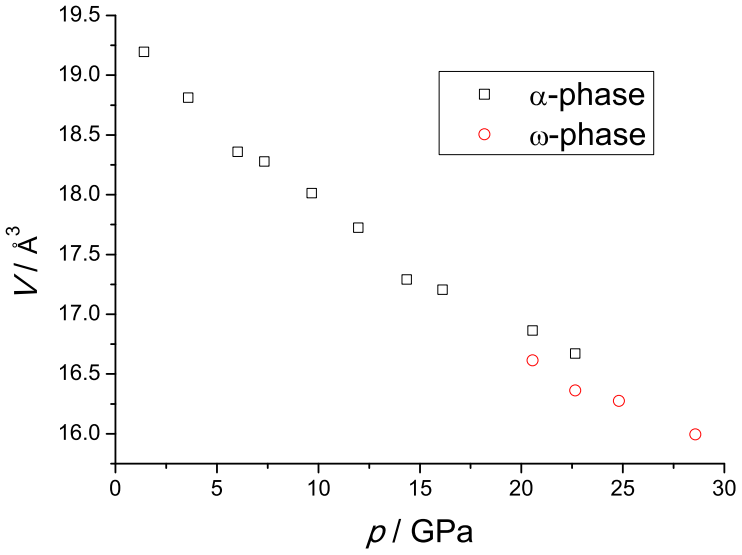

Figure 5. The pressure dependence in $Ti_{0.676}Zr_{0.324}$ of the atomic volume V for the α-phase [open (black) squares] and for the ω-phase [open (red) circles]. The error bars are smaller than the symbol sizes.

Eulerian strain, V_0 and B_0 are the atomic volume and isothermal bulk modulus at zero pressure, respectively, and B_0' is the pressure derivative of the isothermal bulk modulus at zero pressure. A plot of F_E versus f_E enables B_0 and B_0' to be obtained from a least-squares fit of the data to a straight line, and an incorrect value for V_0 will manifest itself by an abnormal curvature in the plotted data points at small f_E values [27]. Thus, fitted parameter values of $V_0 = 19.50(15)$ Å^3, $B_0 = 87.1(3.7)$ GPa and $B_0' = 6.58(81)$ were obtained. The zero-pressure volume compares to an ambient pressure value of 19.56(2) Å^3

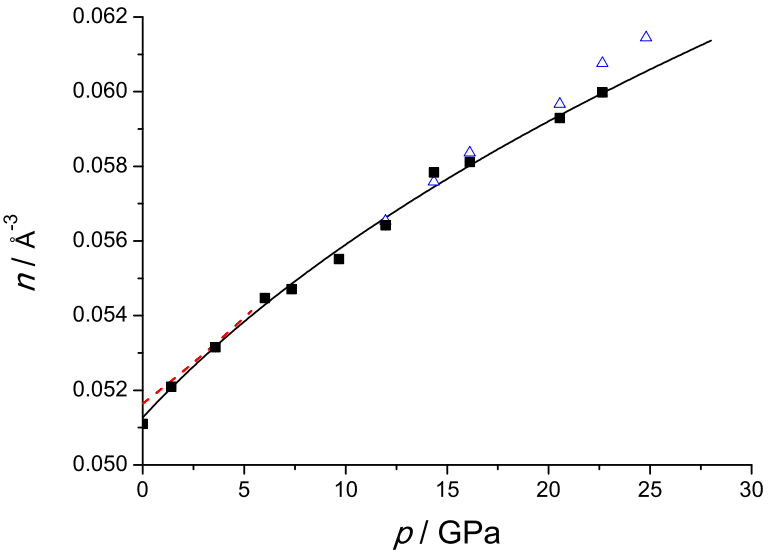

Figure 6. The pressure dependence of the atomic number density n in $Ti_{0.676}Zr_{0.324}$ for (i) the α-phase [filled (black) squares] and (ii) the average of the α- and ω-phases in their coexistence region [open (blue) triangles]. The error bars are smaller than the symbol sizes. The solid curve gives the values of n obtained for the α-phase from a fitted third order Birch-Murnaghan equation of state. The broken curve shows the expectation of Vegard's law for the number density of α-$Ti_{0.676}Zr_{0.324}$ at pressures $\lesssim$5.5 GPa, as calculated by using the measured cell parameters for α-Ti [25] and α-Zr [29] (see the text).

(corresponding to a mass density of 5.257(6) g/cm^3) that was measured by using a MICRO-ULTRAPYC 1200e He gas pycnometer.

The pressure dependence of the measured atomic number density n for the $Ti_{0.676}Zr_{0.324}$ alloy is shown in Figure 6, along with the values obtained for the α-phase from the fitted Birch-Murnaghan equation of state. The results for the α-phase at pressures $\lesssim$5.5 GPa are compared to those expected from Vegard's law [28] where, at a particular pressure, the lattice parameters for an alloy of composition Ti_xZr_{1-x} ($0 \leq x \leq 1$) are taken to be $a = xa_{Ti} + (1-x)a_{Zr}$ and $c = xc_{Ti} + (1-x)c_{Zr}$. In these expressions, a_{Ti} and c_{Ti} are the lattice parameters for α-Ti [25], and a_{Zr} and c_{Zr} are the lattice parameters for α-Zr [29]. For the hcp α-phase of a Ti_xZr_{1-x} alloy, two atoms are contained within a unit cell of volume $V_{cell} = \left(\sqrt{3}/2\right) a^2c$. The number densities thus calculated for α-$Ti_{0.676}Zr_{0.324}$ are consistent with the equation of state values to within a fractional error of $<$1%.

4. Discussion

The bulk moduli measured for the α-phases of Ti, $Ti_{0.676}Zr_{0.324}$, $Ti_{0.5}Zr_{0.5}$ and Zr are compared in Table 1. For a given material, there is a spread in values that may originate from factors such as the sample purity and grain size. For example, the rigidity and hardness of Ti increases with oxygen content as its breaking-strain decreases [33], while the grain size can affect stress distributions and deformation mechanisms during compression [24]. It is notable that precipitation of the ω-phase in Ti and Zr alloys can also have a marked impact on their mechanical properties [34].

As shown in Table 1, the variation in B_0 values for the end members, namely 102–117 GPa for Ti versus 83–94.8 GPa for Zr, is much less than the discrepancy in values reported for the alloys, i.e. $B_0 = 87(4)$ GPa for $Ti_{0.676}Zr_{0.324}$ versus $B_0 = 148(3)$ GPa for

Material	B_0 / GPa	B'_0	Reference
Ti	102	9.1	[30]
Ti	105	–	[31]
Ti	106.69	4.54	[24][a]
Ti	114(3)	4	[25]
Ti	117(9)	3.9(4)	[23]
$Ti_{0.676}Zr_{0.324}$	87(4)	6.6(8)	present work
$Ti_{0.5}Zr_{0.5}$	148(3)	3.8(2)	[21]
Zr	83	–	[31]
Zr	92(3)	4	[29]
Zr	94.8	4.11	[32]

Table 1. The zero-pressure isothermal bulk modulus and its first pressure derivative for the α-phases of Ti, $Ti_{0.676}Zr_{0.324}$, $Ti_{0.5}Zr_{0.5}$ and Zr. [a] Nano-crystalline material.

$Ti_{0.5}Zr_{0.5}$. In the compression experiments on these alloys, the onset of the $\alpha \rightarrow \omega$ phase transition was observed at $\lesssim$12 GPa for the null-scattering alloy versus 11.0(1.5) GPa for the equiatomic $Ti_{0.5}Zr_{0.5}$ alloy in the work by Bashkin et al. [21], where the latter was deduced by comparing data from energy dispersive x-ray diffraction and super-conducting transition temperature measurements. There is not, therefore, a clear correlation between the difference in B_0 values for these alloys and the pressure at which the ω-phase first starts to appear. The role played by impurities is difficult to assess because they were not identified specifically in work on the equiatomic $Ti_{0.5}Zr_{0.5}$ alloy: The impurity content of the starting elements Ti and Zr was given as <0.02 and <0.04 at.%, respectively, and electron microprobe analysis indicated a final alloy with 49.6 at.% Ti and 50.4 at.% Zr, with an uncertainty of $\pm$0.4 at.% [21, 22].

It would therefore be helpful to make a systematic investigation on the influence of factors such as oxygen content, grain size and precipitation of the ω-phase on the mechanical properties of Ti_xZr_{1-x} alloys. Similarly, given the role played by the null-scattering alloy as a gasket material in high-pressure neutron scattering experiments, it would be helpful to make a systematic assessment of the effect of non-uniform stress on the mechanical properties of this alloy for the different toroidal-anvil geometries that are employed with opposed-anvil setups such as the Paris-Edinburgh press [3]. This information would be useful in modelling the mechanisms of gasket deformation, and may thereby help in avoiding their failure during high-pressure experiments.

5. Conclusion

X-ray diffraction was used to find the pressure-volume equation of state on compression for the 'null-scattering' alloy $Ti_{0.676}Zr_{0.324}$ at room temperature and pressures up to $\sim$30 GPa. An $\alpha \rightarrow \omega$ phase transition was observed over a broad pressure range extending from $\lesssim$12 to $\sim$25 GPa. A third order Birch-Murnaghan equation of state was fitted to the α-phase data, giving a zero pressure isothermal bulk modulus $B_0 = 87(4)$ GPa and a pressure derivative $B'_0 = 6.6(8)$. The results are required for the correction procedures that are employed when analysing the data obtained from *in situ* high-pressure neutron diffraction experiments on amorphous and liquid materials.

6. Acknowledgements

We thank Robert Done (ISIS, UK) and Burkhard Annighöfer (CEA, France) for useful discussions on the properties of Ti-Zr alloys, and Keiron Pizzey (Bath) for helpful discussions on the Birch-Murnaghan equations of state. AZ and PSS were supported by the Engineering and Physical Sciences Research Council (EPSRC) via Grant No. EP/J009741/1. MG was fully supported by EFree, an Energy Frontier Research Center funded by the US Department of Energy (DOE) and Office of Science Basic Energy Sciences (BES) program under award DE-SC0001057. Data collection was conducted at HPCAT (Sector 16), Advanced Photon Source (APS), Argonne National Laboratory, USA. HPCAT operations are supported by the DOE and National Nuclear Security Administration (NNSA) under Award No. DE-NA0001974 and by DOE-BES under Award No. DE-FG02-99ER45775, with partial instrument funding from the National Science Foundation (NSF). Use of the COMPRES-GSECARS gas loading system was supported by COMPRES under NSF Cooperative Agreement No. EAR 11-57758, and by GSECARS through NSF Grant No. EAR-1128799 and DOE Grant No. DE-FG02-94ER14466. APS is supported by DOE-BES under Contract No. DE-AC02-06CH11357.

References

[1] Fast JD. The transition point diagram of the zirconium-titanium system. Rec Trav Chim. 1939;58:973–983.
[2] Hansen M. Constitution of Binary Alloys. 2nd ed. New York (NY): McGraw-Hill; 1958.
[3] Klotz S. Techniques in High Pressure Neutron Scattering. Boca Raton (FL):CRC Press; 2013.
[4] Sears VF, Neutron scattering lengths and cross sections. Neutron News 1992;3:26–37.
[5] Sidhu SS, Heaton L, Zauberis DD, Campos FP. Neutron diffraction study of titanium-zirconium system. J Appl Phys. 1956;27:1040–1042.
[6] Salmon PS and Zeidler A. Networks under pressure: The development of *in situ* high-pressure neutron diffraction for glassy and liquid materials. J Phys Condens Matter. *in press.*
[7] Fischer HE, Cuello GJ, Palleau P, Feltin D, Barnes AC, Badyal YS, Simonson JM. D4c: A very high precision diffractometer for disordered materials. Appl Phys A. 2002;74:S160–S162
[8] Fischer HE, Barnes AC, Salmon PS. Neutron and x-ray diffraction studies of liquids and glasses. Rep Prog Phys. 2006;69:233–299.
[9] Solozhenko VL, Chernyshev VV, Fetisov GV, Rybakov VB, Petrusha IA. Structure analysis of the cubic boron nitride crystals. J Phys Chem Solids. 1990;51:1011–1012.
[10] Zeidler A, Drewitt JWE, Salmon PS, Barnes AC, Crichton WA, Klotz S, Fischer HE, Benmore CJ, Ramos S, Hannon AC. Establishing the structure of GeS_2 at high pressures and temperatures: A combined approach using x-ray and neutron diffraction. J Phys Condens Matter. 2009;21:474217.
[11] Drewitt JWE, Salmon PS, Barnes AC, Klotz S, Fischer HE, Crichton WA. Structure of GeO_2 glass at pressures up to 8.6 GPa. Phys Rev B. 2010;81:014202.
[12] Salmon PS, Drewitt JWE, Whittaker DAJ, Zeidler A, Wezka K, Bull CL, Tucker MG, Wilding MC, Guthrie M, Marrocchelli D. Density-driven structural transformations in network forming glasses: A high-pressure neutron diffraction study of GeO_2 glass up to 17.5 GPa. J Phys Condens Matter. 2012;24:415102.
[13] Helle AS, Easterling KE, Ashby MF. Hot-isostatic pressing diagrams: New developments. Acta Metall. 1985;33:2163–2174.
[14] Klotz S, Chervin J-L, Munsch P, Le Marchand G. Hydrostatic limits of 11 pressure transmitting media. J Phys D Appl Phys. 2009;42:075413.
[15] Mao HK, Xu J, Bell PM. Calibration of the ruby pressure gauge to 800 kbar under quasi-hydrostatic conditions. J Geophys Res. 1986;91:4673–4676.
[16] Broennimann Ch, Eikenberry EF, Henrich B, Horisberger R, Huelsen G, Pohl E. Schmitt

B, Schulze-Briese C, Suzuki M, Tomizaki T, Toyokawa H, Wagner A. The PILATUS 1M detector, J Synchrotron Rad. 2006;13:120–130.
[17] Hammersley AP. FIT2D: An introduction and overview. ESRF Internal Report, ESRF97HA02T. Grenoble (France):ESRF;1997.
[18] Larson AC, Von Dreele RB. General Structure Analysis System (GSAS). Los Alamos National Laboratory (LANL) Report LAUR 86-748. Los Alamos (NM):LANL;2004.
[19] Sikka S K, Vohra Y K, Chidambaram R. Omega phase in materials. Prog Mater Sci. 1982;27:245–310.
[20] Akahama Y, Kobayashi M, Kawamura H. High-pressure x-ray diffraction study on electronic *s*-*d* transition in zirconium. J Phys Soc Jpn. 1991;60:3211–3214.
[21] Bashkin IO, Fedotov VK, Nefedova MV, Tissen VG, Ponyatovsky EG, Schiwek A, Holzapfel WB. Crystal structure and superconductivity of TiZr up to 57 GPa. Phys Rev B. 2003;68:054401.
[22] Dmitriev VP, Dubrovinsky L, Le Bihan T, Kuznetsov A, Weber H-P, Poniatovsky EG. Collapsed hexagonal ω phase in a compressed TiZr alloy: Angle-dispersive synchrotron-radiation x-ray diffraction study. Phys Rev B. 2006;73:094114
[23] Errandonea D, Meng Y, Somayazulu M, Häusermann D. Pressure-induced $\alpha \rightarrow \omega$ transition in titanium metal: A systematic study of the effects of uniaxial stress. Physica B. 2005;355:116–125.
[24] Velisavljevic N, Jacobsen MK, Vohra YK. Structural phase stability in nanocrystalline titanium to 161 GPa. Mater Res Express. 2014;1:035044.
[25] Zhang J, Zhao Y, Hixson RS, Gray GT III, Wang L, Utsumi W, Hiroyuki S, Takanori H. Thermal equations of state for titanium obtained by high pressure-temperature diffraction studies. Phys Rev B. 2008;78:054119.
[26] Xia H, Duclos SJ, Ruoff AL, Vohra YK. New high-pressure phase transition in zirconium metal. Phys Rev Lett. 1990;64:204–207.
[27] Angel RJ. Equations of State. In: Hazen RM, Downs RT, editors. High-Temperature and High-Pressure Crystal Chemistry (Reviews in Mineralogy and Geochemistry vol 41, chapter 2): Chantilly (VA): Mineralogical Society of America; 2000. p. 35–59.
[28] Vegard L. Die Konstitution der Mischkristalle und der Raumfüllung der Atome. Z Phys. 1921;5:17–26.
[29] Zhao Y, Zhang J, Pantea C, Qian J, Daemen LL, Rigg PA, Hixson RS, Gray GT III, Yang Y, Wang L, Wang Y, Uchida T. Thermal equations of state of the α, β, and ω phases of zirconium. Phys Rev B. 2005;71:184119.
[30] Vohra YK, Spencer PT. Novel γ-phase of titanium metal at megabar pressures. Phys Rev Lett. 2001;86:3068–3071.
[31] Gschneidner KA Jr. Physical properties and interrelationships of metallic and semimetallic elements. Sol State Phys. 1964;16:275–426.
[32] Fisher ES, Manghnani MH, Sokolowski TJ. Hydrostatic pressure derivatives of the single-crystal elastic moduli of zirconium. J Appl Phys. 1970;41:2991–2998.
[33] Lison R. Schweissen und Löten von Sondermetallen und ihren Legierungen [Welding and Brazing of Special Metals and their Alloys]. Fachbuchreihe Schweißtechik [Textbook Series in Welding Techniques] Band 118. Düsseldorf (Germany): Deutscher Verlag für Schweisstechnik DVS-Verlag GmbH; 1996.
[34] Hickman BS. The formation of omega phase in titanium and zirconium alloys: A review. J Mater Sci. 1969;4:554–563.